



Special Feature: CAE and Simulation

Research Report

Topology Optimization Utilizing Automated Solutions of Partial Differential Equations

Atsushi Kawamoto, Tadayoshi Matsumori, Tsuguo Kondoh and Tsuyoshi Nomura

Report received on Nov. 20, 2014

■ABSTRACT■ The present paper deals with topology optimization in terms of practical implementation utilizing automated solutions of partial differential equations (PDE). First, the theoretical background of topology optimization is reviewed, and an issue inherent to the regularization of the design space is discussed. Using a Heaviside projection-based representation, a PDE-based filtering technique is presented so as to directly act on the design variables and preserve the consistency of the design sensitivities. Moreover, a time evolution equation is presented to solve topology optimization problems using the standard BDF method with an adaptive time step scheme. All programs are implemented in COMSOL Multiphysics. From an agility point of view, the proposed methods are advantageous because all of the necessary elements are already included in the software package. Therefore, the proposed methods can be implemented simply by describing equations. The effectiveness of the proposed methods is confirmed through stiffness maximization problems with a total volume constraint. Moreover, the practicality of the time evolution scheme is demonstrated through its application to the structural design of a lightweight car seat.

■KEYWORDS■ Topology Optimization, Heaviside Projection Method, Time-dependent Diffusion Equation, Regularization, Compliance Minimization

1. Introduction

Topology optimization is a mathematical design method that cannot only optimize the sizes and dimensions but also the shapes and topologies of structures.^(1,2) The essence of topology optimization is to transform structural design problems into material distribution problems. Structural designs are represented by a scalar function called the characteristic function that takes a value of either 0 or 1, where 0 indicates a void and 1 indicates a solid. Using this representation, complicated layouts of target structures can be freely designed by distributing materials. However, this representation may cause some numerical instability due to a lack of smoothness in the characteristic function. In order to regularize the design spaces, the characteristic function is first relaxed so as to take intermediate values between 0 and 1. Then, typically, either a convolution filtering technique or perimeter control is applied.

On the other hand, the recent development of automated solutions of partial differential equations (PDE) is also notable. Automated software packages have recently become available, both commercially

and non-commercially. Both COMSOL Multiphysics (commercial) and FEniCS⁽³⁾ (non-commercial) seek to automate the solution of differential equations based on the finite element method. The implementation of the finite element method itself is a formidable task, but it is completely automated and hidden behind the formulation in these automated systems. All that is needed is to write expressions for solving partial differential equations.

In the context of topology optimization, automated systems are useful for solving known and unknown physical problems. Furthermore, by incorporating filtering techniques and optimization methods into relevant forms of partial differential equations, automated solution systems may also provide an interesting opportunity to assist with the agile development of topology optimization.

In the present paper, we focus on powerful but less widely used regularization and optimization methods utilizing automated solutions of partial differential equations. We discuss the effectiveness and advantages of the proposed methods through numerical examples.

2. Topology Optimization

This section provides a brief introduction to the topology optimization method and some inherent issues in the methodology. **Figure 1** shows the design domain with the boundary and load conditions for a benchmark design problem, in which we maximize the stiffness of a cantilever beam by distributing a prescribed amount of material within the design domain. This problem can be formulated as the minimization of the mean compliance under the total volume constraint:

$$\begin{aligned} & \underset{\varepsilon \leq \rho \leq 1}{\text{minimize}} && f := \int_{\Gamma_N} \mathbf{t} \cdot \mathbf{u} \, d\Gamma, \\ & \text{subject to} && g := \int_D \rho \, dD - \bar{V}. \end{aligned} \tag{1}$$

Note that the design variables are relaxed so as to take intermediate values between ε and 1, where ε ($= 0.01$) is the lower bound set in order to avoid a singularity in void regions. The displacement vector, \mathbf{u} , is calculated from the following analysis problem:

$$\left. \begin{aligned} -\nabla \cdot \boldsymbol{\sigma} &= \mathbf{0} && \text{in } D \\ \mathbf{u} &= \mathbf{0} && \text{on } \Gamma_D \\ \mathbf{n} \cdot \boldsymbol{\sigma} &= \mathbf{t} && \text{on } \Gamma_N \end{aligned} \right\}. \tag{2}$$

Assuming infinitesimal deformation, the stress tensor $\boldsymbol{\sigma}$ is expressed in terms of a homogeneous isotropic elasticity tensor \mathbf{E} and a linear strain tensor $\boldsymbol{\epsilon}$ as follows:

$$\boldsymbol{\sigma} = \mathbf{E} : \boldsymbol{\epsilon}(\mathbf{u}), \quad \boldsymbol{\epsilon}(\mathbf{u}) = \frac{1}{2} (\nabla \mathbf{u} + \nabla \mathbf{u}^T). \tag{3}$$

The material density ρ is embedded in the elasticity

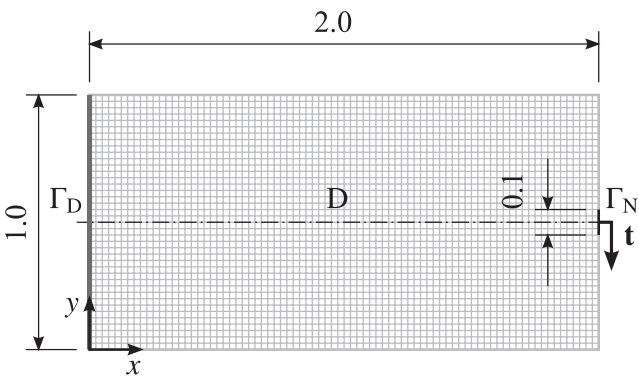


Fig. 1 Design domain and boundary conditions for a cantilever beam design problem.

tensor as

$$\mathbf{E} = \rho^P \mathbf{E}_{\max}, \tag{4}$$

where \mathbf{E}_{\max} is the elasticity tensor of the solid material, i.e., $\mathbf{E} = \mathbf{E}_{\max}$ when $\rho = 1$. P ($= 3$; typically) is introduced to promote black and white solutions.⁽²⁾ The design domain is discretized by a square element of length $\Delta x = 0.025$. In this problem, we pursue a symmetric design. Therefore, we only solve half of the domain. This problem can be solved using a continuous gradient-based optimization method, such as SNOPT.⁽⁴⁾ The design sensitivities are available via the standard adjoint-based sensitivity analysis.⁽²⁾ The results are shown in **Fig. 2**. In the left illustration a large gray area (grayscale problem) remains. By increasing the value of P we can force the design variables toward 0 or 1. However, we typically end up with a solution such as that indicated on the right-hand side of Fig. 2 (checkerboard problem).

3. PDE-based Regularization⁽⁵⁾

Since the density function, $\rho \in L^\infty(D)$, can take any point-wise value, the raw density function may produce severely oscillating designs, such as the checkerboard pattern shown in the right illustration of Fig. 2.

In order to mitigate the numerical instability, thus far, several image-processing based filtering techniques have been proposed. These techniques are conventionally applied to the design sensitivities rather than the design variables themselves. However, this causes discrepancies between the filtered sensitivities and the actual sensitivities that may confuse the optimization process and disturb the convergence. Here we instead propose a Heaviside projection-based topology optimization method⁽⁶⁾ with a scalar function that is filtered by a Helmholtz-type partial differential equation. Therefore, the optimality can be strictly discussed in terms of the KKT condition. In order to regularize the density function we first introduce an intermediate mathematical design variable ϕ and the

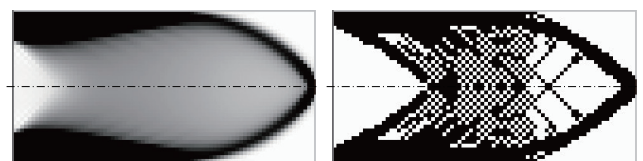


Fig. 2 Optimized structures for $P = 1$ (left) and $P = 3$ (right).

following partial differential equation for $\varphi \in H^1(D)$:

$$-R^2 \nabla^2 \varphi + \varphi = \phi. \quad (5)$$

This equation simply substitutes ϕ into φ when the first term is canceled, i.e., $R = 0$. On the other hand, the equation becomes Poisson's equation when $R \rightarrow \infty$. By appropriately setting R to an intermediate value, this equation functions as a low pass filter that acts on a raw scalar function ϕ to produce the smoothed scalar function φ . The investigation of the associate Green function clarifies this function.⁽⁷⁾ **Figure 3** shows the shape of the Green function for the case in which R is set to 0.5 and the Neumann condition is applied to all four boundaries. Here, φ can be expressed by the convolution integral of the Green function multiplied by the input ϕ . In other words, we seek the optimum design within the space of smoothed φ restricted by the equation.

Then, we project φ onto ρ as follows:

$$\rho(\varphi) = \begin{cases} \varepsilon & (\varphi < -h), \\ \frac{1}{2} + \frac{15}{16} \left(\frac{\varphi}{h}\right) - \frac{5}{8} \left(\frac{\varphi}{h}\right)^3 + \frac{3}{16} \left(\frac{\varphi}{h}\right)^5 & (-h \leq \varphi \leq h), \\ 1 & (h < \varphi), \end{cases} \quad (6)$$

where h is a positive parameter for the bandwidth between the complete material domain (where $h < \varphi$) and the complete void domain (where $\varphi < -h$). Therefore, the bandwidth is equal to $2h$. Finally we

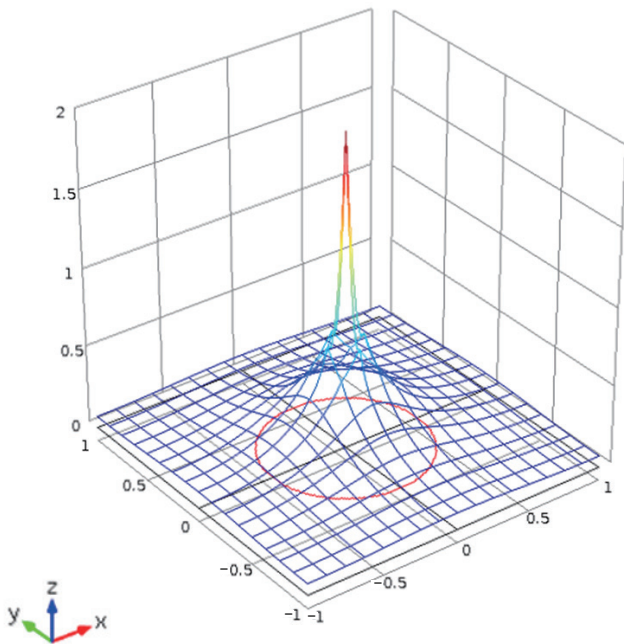


Fig. 3 Green function of Eq. (5) under the Neumann condition.

use the projected smooth density function, ρ , for the material interpolation in Eq. (4) instead.

In order to solve the optimization problem of Eq. (1) for the new design variable, ϕ , (instead of ρ), we seek the following first-order necessary condition for the Lagrange function $L := f + \lambda g$, i.e., the KKT condition:

$$\frac{dL}{d\phi} = \frac{df}{d\phi} + \lambda \frac{dg}{d\phi} = 0, \lambda g = 0, \lambda \geq 0, g \leq 0, \quad (7)$$

where λ is the Lagrange multiplier.

Figure 4 illustrates the optimized results for the density in grayscale for the case in which parameter R in the partial differential Eq. (5) is set to $\{1.0 \Delta x; 2.0 \Delta x; 4.0 \Delta x\}$, and the half-bandwidth, h , in the projection of Eq. (6) is set to $\{0.1; 0.5; 1.0\}$. The lesser R and the tighter h (the upper left) give finer details with a clear outline in the final design, whereas the opposite combination (lower right) makes the outline extremely blurred. Note that, in all cases, no checkerboard patterns appeared even though the linear elements are used for the discretization.

Figure 5 shows the histories of the objective function and the relative complementarity gap for the case in which $R = 1.5 \Delta x$ and $h = 0.5$. The complementarity gap indicates how well the KKT condition of Eq. (7) is satisfied. In this particular case, assuming the j -th component of the reduced gradient as

$$d_j = \frac{\partial f}{\partial \phi_j} + \lambda \frac{\partial g}{\partial \phi_j}, \quad (8)$$

the complementarity gap e is equivalently defined as

$$e = \max_j s_j / \|\lambda\|, \quad (9)$$

where

$$s_j = \begin{cases} -d_j \min \{1 - \phi_j, 1\} & (d_j \leq 0), \\ d_j \min \{\phi_j + 1, 1\} & (d_j > 0). \end{cases} \quad (10)$$

The optimization process is terminated when the complementarity condition is satisfied within the tolerance as $e \leq 10^{-5}$ (called optimality tolerance in SNOPT⁽⁴⁾). In this case the optimization converged after 45 iterations.

Incidentally, the proposed regularization scheme can be applied to the level set based approach, for instance, and of course other types of physics.⁽⁸⁾

4. PDE-based Topology Optimization⁽⁹⁾

Alternatively one can solve the minimum compliance










	$R = 1.0 \Delta x$	$R = 1.5 \Delta x$	$R = 2.0 \Delta x$
$h = 0.1$	 $f = 0.2025, \text{Iter.}: 57$	 $f = 0.2033, \text{Iter.}: 56$	 $f = 0.2042, \text{Iter.}: 47$
$h = 0.5$	 $f = 0.2095, \text{Iter.}: 35$	 $f = 0.2161, \text{Iter.}: 45$	 $f = 0.2193, \text{Iter.}: 34$
$h = 1.0$	 $f = 0.2262, \text{Iter.}: 46$	 $f = 0.2402, \text{Iter.}: 34$	 $f = 0.2501, \text{Iter.}: 29$

Fig. 4 Optimized results using the PDE-based filtering technique.

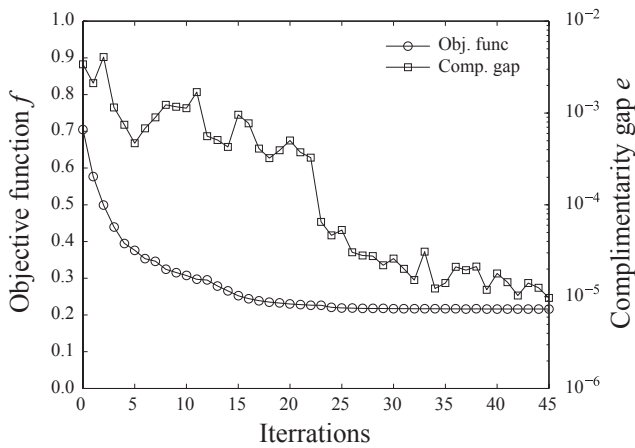


Fig. 5 Optimization histories.

problem using time evolution equations. If the correct value of the Lagrange multiplier, λ^* , is somehow provided, the constrained optimization problem (1) can be solved by simply minimizing the Lagrange function L as an unconstrained optimization problem. In order to penalize the violation of the volume constraint, the Lagrange multiplier is modified as follows:

$$\lambda = \begin{cases} 0 & (\lambda^* \leq 0), \\ \lambda^* \exp(\beta g) & (\lambda^* > 0), \end{cases} \quad (11)$$

where β is a positive parameter for controlling the

violation of the constraints.

With the reduced gradient in Eq. (7) modified as

$$\frac{\widehat{dL}}{d\phi} = \frac{df}{d\phi} / \int_D \left| \frac{df}{d\phi} \right| dD + \lambda \frac{dg}{d\phi} / \int_D \left| \frac{dg}{d\phi} \right| dD \quad (12)$$

into the source term, we finally use the following time-dependent diffusion equation for searching the solution:

$$\frac{\partial \phi}{\partial t} = \kappa \nabla^2 \phi - \alpha \frac{\widehat{dL}}{d\phi}, \quad (13)$$

where the first term on the right hand side with the positive parameter κ gives a diffusion effect for regularizing (smoothing) the function ϕ . Note that, in the current situation, in which the volume constraint is active in the end, the Lagrange multiplier can be fixed as $\lambda^* = 1$ because the objective and constraint functions are both normalized.

The main flow of the computation is summarized in **Table 1**. **Table 2** describes the parameters and the default values adopted in the algorithm. For solving the partial differential Eq. (13) in time, we apply the standard backward differentiation formula (BDF) method with an adaptive time step scheme.⁽¹⁰⁾ All of the programs are implemented in COMSOL Multiphysics. From an implementation point of view, the proposed method is advantageous because all of the necessary elements are already included in the software package.

Table 1 Algorithm for topology optimization.

1)	Set all constants: $\alpha, \beta, \kappa, \varepsilon P$.
2)	Set initial values for ϕ .
3)	Calculate ρ by Eq. (6).
4)	Solve the forward problem of Eq. (2).
5)	Calculate the sensitivities in Eq. (9).
6)	Determine the modified Lagrange multiplier λ by Eq. (8).
7)	Update the design variables ϕ by Eq. (10).
8)	Return to 2) for next time step, or terminate if a stopping criterion is met.

Table 2 Parameters and default values.

Parameters	Values
Lower bound for the material density in Eq. (6): ε	0.01
Half bandwidth in Eq. (6): h	1.0
Source term coefficient in Eq. (10): α	0.1
Parameter for modifying Lagrange multipliers in Eq. (8): β	2.0
Diffusion coefficient in Eq. (10): κ	1.0^{-4}

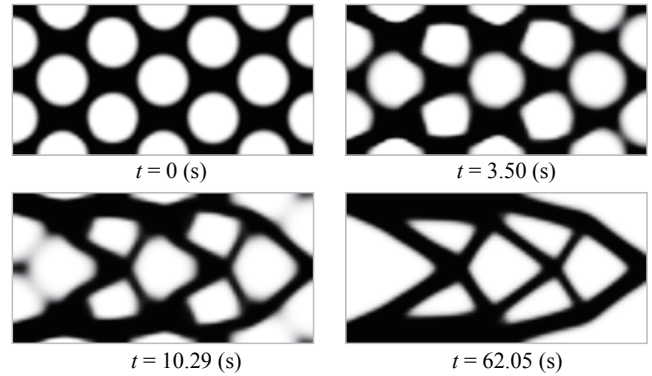


Fig. 6 Optimization process of the material density distribution solved by the time evolution equation.

Therefore, the proposed method can be implemented by simply describing equations, i.e., programming using the Matlab interface is not required.⁽¹¹⁾

Figure 6 provides snapshots of the optimization process, showing the material densities, at $t = 0, 3.50, 10.29$ and 62.05 . Since the design sensitivities are restricted by the Heaviside function of Eq. (6) within the interface boundaries, the initial black and white configuration may produce a similar boundary tracking behavior to that of the level set methods. **Figure 7** shows the optimization histories of the objective function on the left, the volume constraint in the center and the Lagrange multiplier on the right.

In order to demonstrate the practicality of the proposed method for solving large scale problems, a

lightweight car seat structure design problem is solved. The left-hand side of **Fig. 8** shows the design domain. A symmetric seat is pursued here so the design domain is only the half of the entire domain divided by the symmetry plane of $y = 0$. The right-hand side shows the mesh, which is composed of 1,928,074 tetrahedrons with a maximum length of less than 0.005 m. The state and design fields are both discretized using the Lagrange linear shape functions. The total number of degrees of freedom is 1,371,832: 1,028,874 degrees of freedom for the state variables and 342,958 degrees of freedom for the design variables. In order to simulate a seated passenger, a homogeneous pressure load is exerted on the surface of the seat, depicted in gray on the left-hand side of **Fig. 9**. Considering the inclination of the seat back, 1/3 of the homogeneous pressure load is exerted on the surface of the seat back depicted in gray in the center panel of **Fig. 9**. For fixing the seat structure, equivalent counter forces are exerted on the candidate fixing positions within the gray area on the

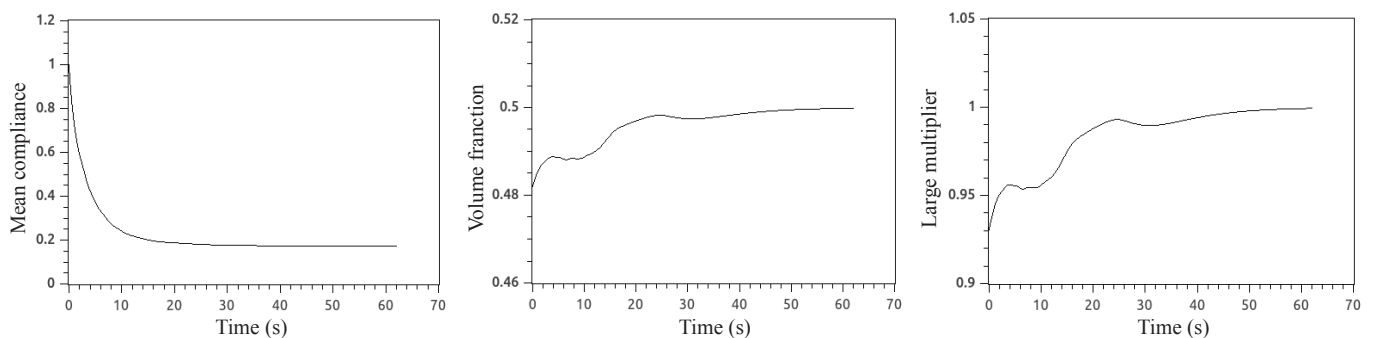


Fig. 7 Optimization histories: objective function, normalized by the initial value (left); volume constraint, normalized by the area of the design domain (center); Lagrange multiplier (right).

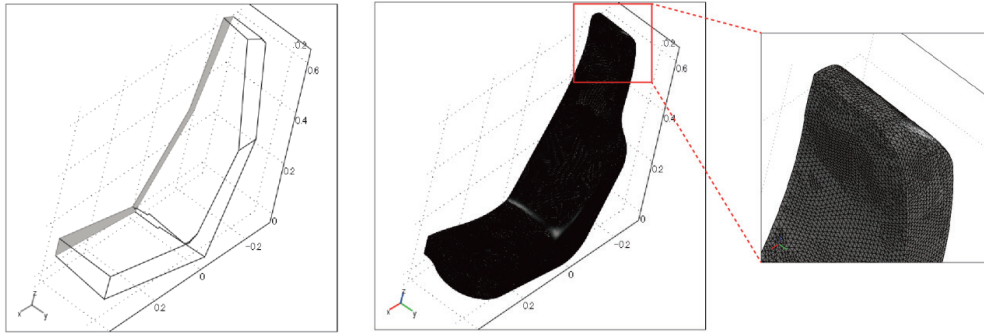


Fig. 8 Symmetric design domain (left); FEM mesh (right).

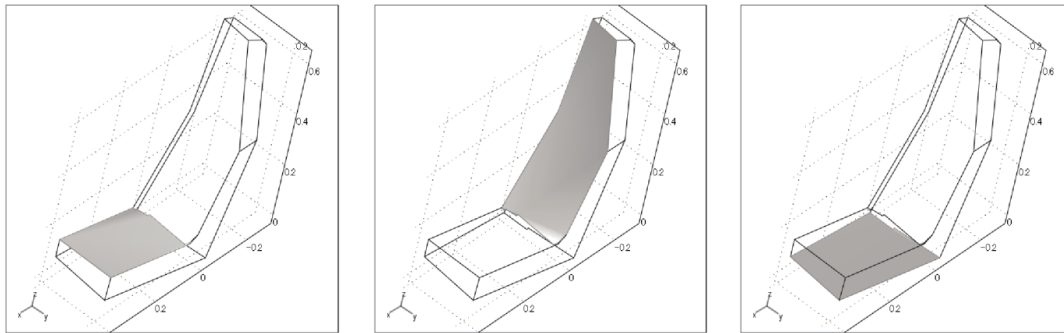


Fig. 9 Load condition: seat (left), back (center), fixing (right).

right-hand side of Fig. 8.

The upper bound of the total volume fraction is set to 15% of the entire design domain. The initial value for ϕ is set to zero everywhere. The time integration of Eq. (10) is conducted to the convergence until $t = 5$ s. All computations are performed on a computer with four CPUs (2.93 GHz Intel (R) Xeon) and 64 GB RAM. The PARDISO direct solver computing library is used for solving linear systems of equations. The total computation time is approximately 5 days, which is much shorter than the time (weeks or more) required by the conventional mathematical programming approach.

Figures 10 (front view) and **11** (rear view) provide the snapshots of the optimization history, including the isosurface of the material density $\rho = 0.1$. In the figures, the initial, intermediate, and final designs are shown on the left, in the center, and on the right, respectively.

5. Conclusions

We revisited the theoretical background of topology optimization and discussed the issues inherent to

the regularization in topology optimization. Using a Heaviside projection-based representation, we presented a PDE-based filter that acts directly on the design variables. Thus, the consistency of the design sensitivities is preserved. Moreover, we presented a time evolution equation that solves topology optimization problems using the standard BDF method with an adaptive time step scheme. All programs were implemented in COMSOL Multiphysics. From an agility point of view, the proposed methods are advantageous because all of the necessary elements are already included in the software package. Therefore, the proposed methods can be implemented simply by describing equations without using the MATLAB interface. The effectiveness of the proposed methods was confirmed through stiffness maximization problems with a total volume constraint. Moreover, the practicality of the time evolution scheme was demonstrated by its application to the lightweight car seat structural design problem. Although FEniCS could be an alternative to COMSOL Multiphysics, FEniCS is not as easy to use as COMSOL Multiphysics, due to the lack of a GUI.

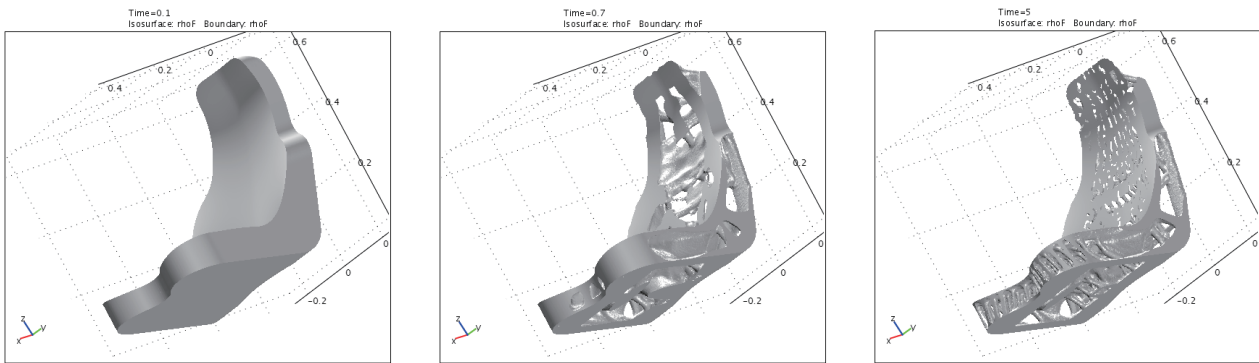


Fig. 10 Optimization history (front view): initial shape (left), intermediate shape (center), final shape (right).

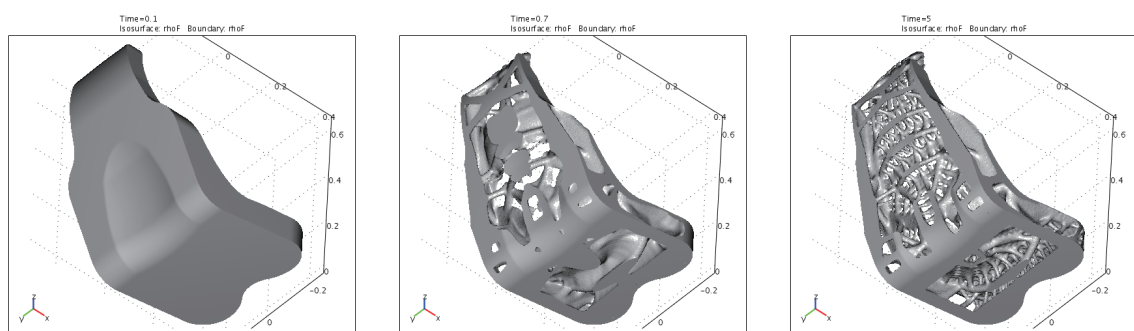


Fig. 11 Optimization history (rear view): initial shape (left), intermediate shape (center), final shape (right).

References

- (1) Bendsøe, M. P. and Kikuchi, N., "Generating Optimal Topologies in Structural Design Using a Homogenization Method", *Comput. Methods Appl. Mech. Eng.*, Vol. 71, No. 2 (1988), pp. 197-224.
- (2) Bendsøe, M. P. and Sigmund, O., *Topology Optimization; Theory, Methods, and Applications* (2003), 370p., Springer.
- (3) Logg, A., Mardal, K.-A. and Wells, G. N., *Automated Solution of Differential Equations by the Finite Element Method* (2012), 723p., Springer.
- (4) Gill, P. E., Murray, W. and Saunders, M. A., *User's Guide for SNOPT Version 7: Software for Large-scale Nonlinear Programming* (2007), Dept. of Mathematics, Univ. of California.
- (5) Kawamoto, A., Matsumori, T., Yamasaki, S., Nomura, T., Kondoh, T. and Nishiwaki, S., "Heaviside Projection Based Topology Optimization by a PDE-filtered Scalar Function", *Struct. Multidiscipl. Optim.*, Vol. 44, No. 1 (2011), pp. 19-24.
- (6) Guest, J. K., Prevost, J. H. and Belytschko, T., "Achieving Minimum Length Scale in Topology Optimization Using Nodal Design Variables and Projection Functions", *Int. J. Numer. Methods Eng.*, Vol. 61, No. 2 (2004), pp. 238-254.
- (7) Lazarov, B. S. and Sigmund, O., "Filters in Topology Optimization Based on Helmholtz-type Differential Equations", *Int. J. Numer. Methods Eng.*, Vol. 86, No. 6 (2011), pp. 765-781.
- (8) Yamasaki, S., Nomura, T., Kawamoto, A., Sato, K. and Nishiwaki, S., "A Level Set-based Topology Optimization Method Targeting Metallic Waveguide Design Problems", *Int. J. Numer. Methods Eng.*, Vol. 87, No. 9 (2011), pp. 844-868.
- (9) Kawamoto, A., Matsumori, T., Yamasaki, S., Nomura, T., Kondoh, T. and Nishiwaki, S., "Topology Optimization by a Time-dependent Diffusion Equation", *Int. J. Numer. Methods Eng.*, Vol. 93, No. 8 (2013), pp. 795-817.
- (10) Brown, P. N., Hindmarsh, A. C. and Petzold, L. R., "Using Krylov Methods in the Solution of Large-scale Differential-algebraic Systems", *SIAM J. Sci. Comput.*, Vol. 15, No. 6 (1994), pp. 1467-1488.
- (11) Olesen, L. H., Okkels, F. and Bruus, H., "A High-level Programming-language Implementation of Topology Optimization Applied to Steady-state Navier-Stokes Flow", *Int. J. Numer. Methods Eng.*, Vol. 65, No. 7 (2006), pp. 975-1001.

Fig. 1

Reprinted from Int. J. Numer. Methods Eng., Vol. 93, No. 8 (2013), pp. 795-817, Kawamoto, A. et al., Topology Optimization by a Time-dependent Diffusion Equation, © 2013 John Wiley & Sons, with permission from John Wiley & Sons.

Figs. 4 and 5

Reprinted from Struct. Multidiscipl. Optim., Vol. 44, No. 1 (2011), pp. 19-24, Kawamoto, A. et al., Heaviside Projection Based Topology Optimization by a PDE-filtered Scalar Function, © 2011 Springer-Verlag, with permission from Springer-Verlag.

Atsushi Kawamoto

Research Fields:

- Topology Optimization
- Nonlinear Dynamics
- Math Programming

Academic Degree: Ph.D.

Academic Society:

- The Japan Society of Mechanical Engineers

Award:

- JSME Design & Systems Achievement Award, 2014

**Tadayoshi Matsumori**

Research Fields:

- Optimum Design
- Topology Optimization
- Shape Optimization

Academic Degree: Dr.Eng.

Academic Society:

- The Japan Society of Mechanical Engineers

Award:

- JSME Merit for Best Technological Presentation, 2009

**Tsuguo Kondoh**

Research Fields:

- Computational Fluid Dynamics
- Topology Optimization

Academic Degree: Dr.Eng.

Academic Societies:

- The Japan Society of Mechanical Engineers
- The Japan Society for Aeronautical and Space Sciences
- The Japan Society for Industrial and Applied Mathematics

**Tsuyoshi Nomura**

Research Field:

- Topology Optimization

Academic Degree: Ph.D.

Academic Society:

- The Japan Society of Mechanical Engineers

